Journal of Physics: Photonics



OPEN ACCESS

RECEIVED

3 September 2025

13 October 2025

ACCEPTED FOR PUBLICATION

4 November 2025

12 November 2025

Original Content from this work may be used under the terms of the Creative Commons Attribution 4.0 licence.

Any further distribution of this work must maintain attribution to the author(s) and the title of the work, journal citation and DOI.



PAPER

Efficient optical coating design using an autoencoder-based neural network model

Utsa Chattopadhyay^{1,2,*}, Florian Carstens⁵, Morten Steinecke⁵, Tarik Kellermann⁵, Andreas Wienke⁵ D, Ingmar Hartl² D, Nihat Ay^{1,6} D, Christoph M Heyl^{2,3,4} D and Henrik Tünnermann² D

- Institute for Data Science Foundations, Technical University of Hamburg, Blohmstrasse 15, 21079 Hamburg, Germany
- Deutsches Elektronen-Synchrotron DESY, Notkestr. 85, 22607 Hamburg, Germany
- Helmholtz Institute Jena, Fröbelstieg 3, 07743 Jena, Germany
- GSI Helmholtz Centre for Heavy Ion Research, Planckstrasse 1, 64291 Darmstadt, Germany
- Laser Zentrum Hannover e.V., Hollerithallee 8, 30419 Hannover, Germany
- Santa Fe Institute, Santa Fe, NM 87501, United States of America
- Author to whom any correspondence should be addressed.

E-mail: utsa.chattopadhyay@tuhh.de

Keywords: thin film coatings, dielectric coatings, deep learning, optimization

Abstract

Optical thin-film coatings are integral to modern photonics and in particular to ultrafast lasers, providing precise control of dispersion and reflectivity, thus enabling tailored pulse shaping. Designing these coatings represents an inverse problem, requiring the mapping of desired optical properties to physical designs, a task that poses major challenges for traditional heuristic methods, which often rely on time-consuming, expert-guided iteration and can be constrained by the choice of an initial starting point. Here, we present an artificial intelligence (AI) framework for optical thin-film coating design that accelerates the design process, achieving excellent performance characteristics without expert intervention. We discuss our AI approach and demonstrate the capabilities of our algorithm by designing a complex broadband high-reflectivity mirror with state-ofthe-art performance characteristics including a $-200 \, \mathrm{fs}^2$ group delay dispersion covering a spectral range of 940 nm to 1120 nm.

1. Introduction

Optical coatings are indispensable in photonics, playing a critical role in many optical systems, such as lasers, microscopes, and telescopes, as well as everyday items such as eyeglasses and cameras [1, 2]. These coatings are designed to control light by providing high reflectance, specific spectral filter characteristics [3], anti-reflective properties [4], tailored dispersion [5] or polarization characteristics. A thin film or multilayer optical coating functions as an interference structure, where the optical properties are determined by the interference of light waves reflected at the layer interfaces [6, 7].

Despite the well-established analytical solutions for the forward problem, such as the transfer matrix method (TMM) [8] derived from Maxwell's equations [9, 10], the design of optical interference coatings remains a challenging inverse problem. The core challenge is to determine the optimal sequence of materials and layer thicknesses that will produce a desired spectral response. For instance, designing coatings that maintain reflectivity above 99.9% over an extended spectral range while tightly controlling dispersion is a task that typically requires iterative refinements and expert knowledge. This design challenge represents a complex multiobjective optimization problem [11], in particular when multiple optical properties such as reflectivity and group delay dispersion (GDD) must be optimized concurrently to achieve the desired performance. Careful trade-offs are required to balance these objectives, and the complexity increases further when additional parameters such as laser-induced damage threshold (LIDT) [12], electric field strength limitations [13], or manufacturability constraints are considered.

Traditional coating optimization methods, exemplified by the widely used needle algorithm [6, 14], incrementally add, remove, or modify thin layers to optimize optical performance. A significant

challenge with these approaches is their high sensitivity to the initial starting design and the creation and prioritization of the target function, which heavily influences the final outcome of the optimization. Furthermore, these methods require significant computational resources and often rely on expert guidance [15] to select a suitable starting point and navigate the optimization landscape. Each adjustment is evaluated against a merit function, which measures how closely the coating meets the desired optical target properties. Furthermore, evolutionary algorithms [16–19] have been widely used for coating optimization but suffer from slow convergence, making them inefficient for complex designs [11, 20]. More recently, deep learning methods have been explored for optical coating optimization [21–24]. These approaches utilize neural networks trained using pre-existing datasets to predict optical design parameters; however, they typically lack scalability for multiple design requirements and are constrained to specific parameter regimes. Recent advances, such as the work by Jiang and Fan [25], have provided a crucial proof-of-concept by using a generative neural network to design anti-reflection coatings. Although demonstrated in a simplified, single-objective and low-dimensional scenario, their method suggests that generative neural networks could be effectively scaled to address multi-objective and highdimensional design problems. Bridging this gap is critical for complex applications, like optimizing both reflectivity and dispersion of coatings for ultrafast lasers, but requires significant improvements in model generalizability.

Here, we present a novel physics-informed artificial intelligence (AI) framework based on an autoencoder architecture that uses a neural network model to design optical coatings. Unlike traditional optimization techniques, our approach benefits from gradient-based training, which captures complex relationships between reflectivity, dispersion, and multilayer configurations.

A key feature of our model is its physics-informed loss function, which embeds the transfer matrix theory directly into the learning process.

We validate our framework by designing a broadband dispersive mirror, without incorporating expert input or knowledge about existing mirror designs into the design process. Our mirror design reaches performance characteristics that include a reflectivity exceeding 99 % combined with a flat GDD of $-200 \, \mathrm{fs^2}$ across a broad spectral range (940–1120 nm) including material absorption.

2. Methods

The inverse design challenge underlying optical multi-layer coating design is illustrated in figure 1. Designing these optical coatings involves optimizing multilayer structures to achieve specific optical properties, such as high reflectivity or controlled dispersion. However, deriving the required layer structure from the desired properties is a complex inverse problem, traditionally solved using iterative numerical techniques, often combined with expert-guided heuristics. Here, we formulate the optical coating design problem as an inverse problem, where a neural network predicts material layer stacks based on key optical properties such as reflectivity and dispersion. By integrating semi-supervised learning with physics-informed constraints [26], we ensure that the generated designs remain physically valid while optimizing for the desired optical performance. Unlike conventional machine learning approaches that require large labeled datasets, our method does not rely on pre-existing coating designs. Instead, it learns directly from physics-based constraints, allowing efficient and scalable design generation without the need for manually curated training data [15, 27]. This ensures that generated designs adhere to fundamental optical principles, while enabling applicability to previously unexplored parameter spaces.

2.1. Physics-informed autoencoder framework

Our coating-design framework is schematically illustrated in figure 2. We start by encoding the desired optical properties—such as reflectivity and wavelength—into a compact numerical representation using an encoder. This encoded representation is then processed by a decoder to generate the corresponding optical properties, such as reflectivity and dispersion.

In deep learning, an encoder typically maps high-dimensional input data into a lower-dimensional latent space, preserving essential characteristics while enabling efficient reconstruction or prediction of relevant outputs [28, 29]. However, in our case, instead of encoding the input into an abstract latent space, the model directly predicts a physically interpretable parameter set corresponding to the predicted layer stack defined by a set of layer thicknesses. Here and in the following, we assume that each multi-layer stack consists of a predefined number of layers $\ell + 2$, arranged with two different alternating optical refractive index values $n_{1,2}$. This assumption simplifies the inverse design challenge and can be expanded if needed, e.g. by taking more than two materials or a variable number of layers into account. This mapping from optical target properties x, where $x \in \mathcal{X}$, and \mathcal{X} represents the input space, to the

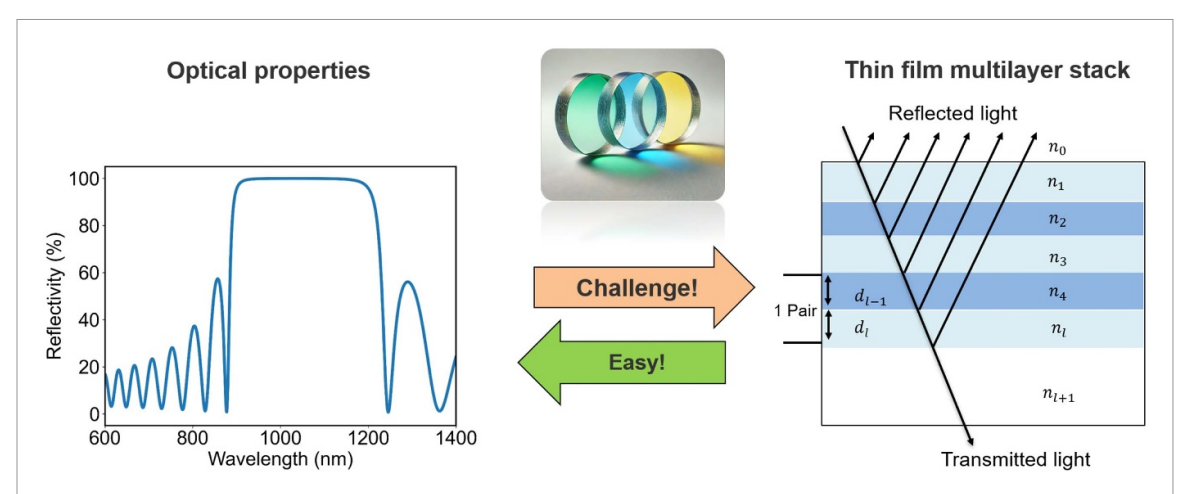


Figure 1. Schematic illustration of the inverse design challenge for optical thin film coatings. While optical properties can be easily and accurately calculated for a given multi-layer stack, the inverse direction, finding a suitable layer stack for a target set of optical properties represents a major challenge. Parts of this figure was created with ChatGPT, using GPT-40 model, (OpenAI).

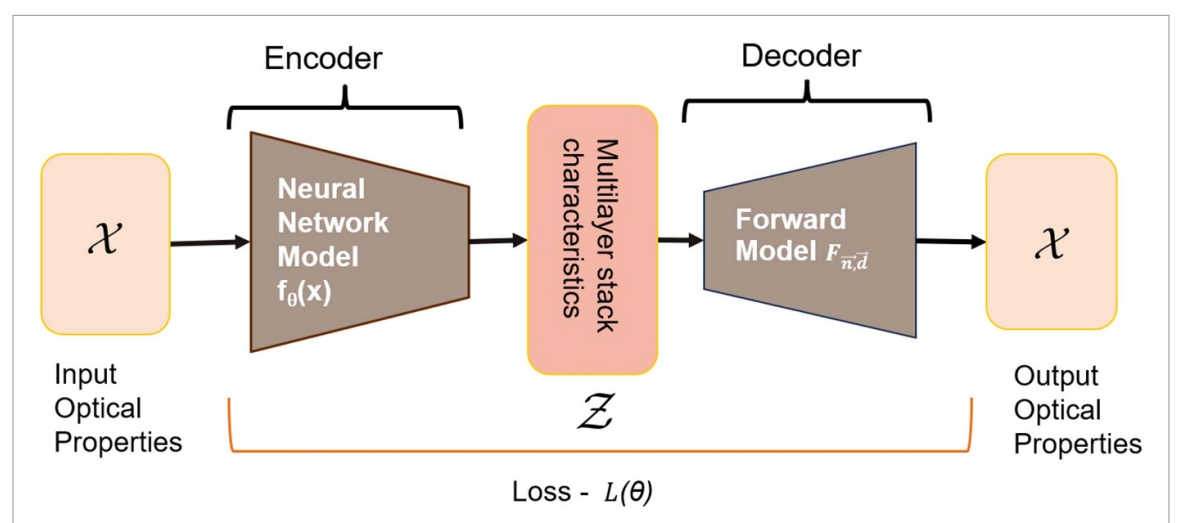


Figure 2. High-level overview of our AI-driven optical coating design framework. The desired optical properties (input) are mapped to a predicted layer stack, and a physics-based forward model reconstructs the optical properties \mathcal{X} .

corresponding physical layer parameters d, where $\vec{d} = (d_0, \dots, d_\ell, d_{\ell+1})$ represents the thicknesses of the stack layers, can be expressed in terms of a predicted internal layer vector z as:

$$z = f_{\theta}(x) = (d_1, \dots, d_{\ell}) \tag{1}$$

where f_{θ} is the neural network of the encoder parameterized by θ , and $z \in \mathbb{R}^{\ell}$ denotes the thicknesses of the ℓ layers. In a conventional autoencoder architecture [28, 29] a trained neural network is used as a decoder, mapping the latent space to an output. In contrast, our approach replaces the decoding step with a physics-based forward model. This model, based on the well-known TMM [8, 30], analytically calculates linear light propagation through multiple interfaces, ensuring the basic principles defined by Maxwell's equations [11]. The TMM uses an index jump matrix, which depends on the refractive indices of adjacent layers and the angle of incidence. The interaction at interfaces and within layers is captured by propagation matrices (T_P) and interface matrices (T_P), leading to a total transformation matrix which can be expressed as:

$$\mathbf{T}_{\text{total}}\left(\vec{n}, \vec{d}, \phi\right) = \mathbf{T}(n_0, n_1) \cdot \mathbf{T}_P(n_1, d_1, \phi) \cdot \mathbf{T}(n_\ell, n_{\ell+1}) \cdot \mathbf{T}_P(n_{\ell+1}, d_{\ell+1}, \phi). \tag{2}$$

Both the propagation and interface matrices depend on the refractive index (\vec{n}) , the thickness of the layer (\vec{d}) , and the incident angle of light (ϕ) . This approach ensures that the neural network does not need to learn the underlying physics of light propagation from existing data sets. Instead, the forward model $(F_{\vec{n},\vec{d}})$ directly enforces physical consistency, as indicated in figure 2.

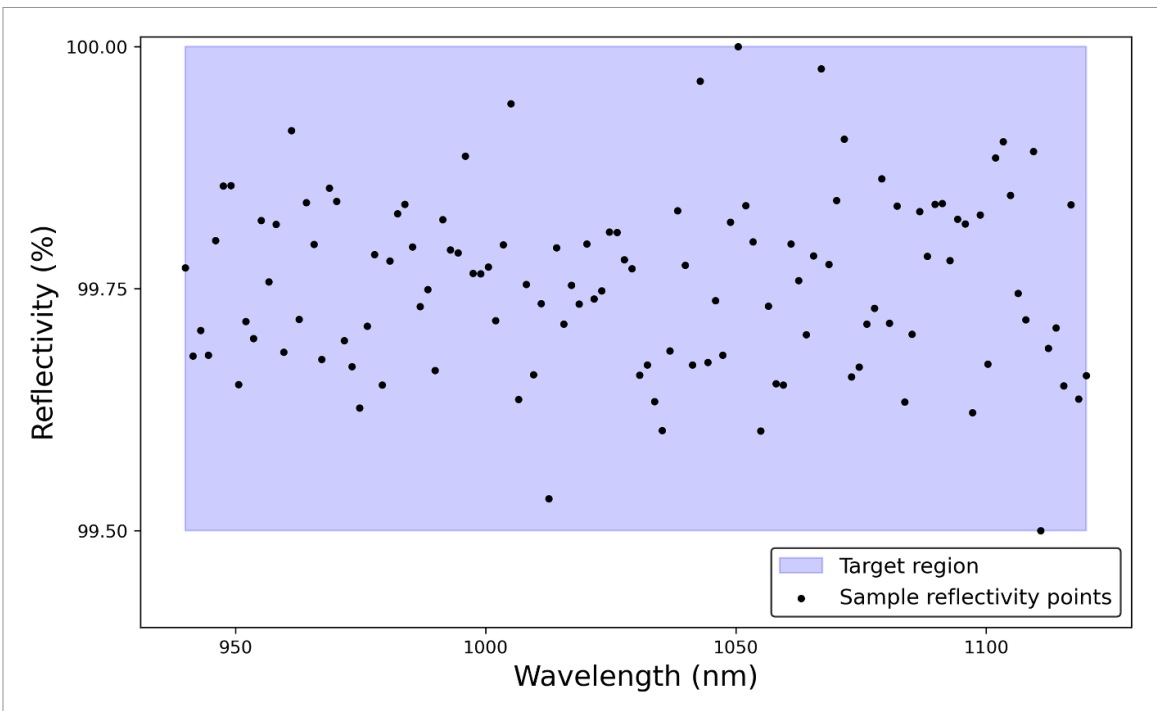


Figure 3. Generated target data: Sample reflectivity data points which are randomly distributed along the reflectivity axis, following a normal distribution centered at 99.75%, truncated to the reflectivity interval and equidistantly distributed along the wavelength axis.

To train our neural network [31], we generate a randomized synthetic dataset of optical properties resembling the targeted coating properties as illustrated in figure 3. This represents a departure from the approach by Jiang and Fan [25], where exploration was initiated using uniformly distributed random values as model inputs. Approximately 500 synthetic samples were generated, ensuring that the network learns the underlying structure of the target reflectivity space (99.5%–100%). The sample count was chosen to balance the diversity of the dataset with computational efficiency. The resulting randomly distributed structured dataset facilitates mapping optical properties to coating designs with satisfactory speed. Further experiments could determine the optimal sample size for improved generalization and stability. The specific hyperparameters for the network architecture and training process are detailed in the supplementary section.

2.2. Optimization objective

Deep neural networks effectively capture a highly non-linear mapping between input and output domains [31], e.g. between optical properties and output material stacks. Our optimization strategy models optical coating design as a minimization problem. The primary goal is to find the optimal set of learnable parameters of the neural network, denoted by θ (i.e. its weights and biases), that minimizes a composite loss function $L(\theta)$. For a chosen example target resembling a chirped mirror, this function simultaneously optimizes reflectivity and GDD. The total loss function can be written as:

$$L(\theta) = L_1(\theta) + \alpha \cdot L_2(\theta). \tag{3}$$

Here, $L_1(\theta)$ represents the reflectivity loss, measuring deviation from the target reflectivity spectrum, and $L_2(\theta)$ is the GDD loss, ensuring the mirror dispersion remains within acceptable limits. The parameter α is a dynamically adjusted weighting factor that governs the trade-off between reflectivity and GDD optimization. We define $L_1(\theta)$ as the mean squared error [26] between the target reflectivity $x_j^{(i)}$ and the predicted reflectivity $\hat{x}_j^{(i)}$ for a given wavelength index j and sample i:

$$L_1(\theta) = \frac{1}{m} \sum_{i=1}^{m} \left(\sum_{j=1}^{n} \left(x_j^{(i)} - \hat{x}_j^{(i)} \right)^2 \right), \tag{4}$$

where m is the total number of training samples (i.e. different synthetic optical targets), as described in 2.1, and n is the number of discrete reflectivity points, as illustrated in figure 3. Each $x^{(i)}$ represents

a full reflectivity spectrum (target) for sample i, and $\hat{x}^{(i)}$ is the predicted spectrum generated from the model. For GDD, instead of using a conventional loss, we apply a penalty function to deviations of GDD beyond a predefined threshold. The penalty is selectively applied only when the GDD deviates beyond an acceptable range, allowing flexibility in minor variations while enforcing strict adherence to constraints for large deviations. The GDD loss can thus be written as:

$$L_{2}(\theta) = \frac{1}{m} \sum_{i=1}^{m} \left(\sum_{k=1}^{p} \max\left(0, |g_{k}^{(i)} - g_{\text{target}}| - t \right) \right). \tag{5}$$

Here, p is the number of GDD features, $g_k^{(i)}$ is the predicted GDD at index k at the sample i, g_{target} is the desired GDD value, and t is the allowable tolerance threshold. The tolerance threshold ensures that minor GDD variations, which do not significantly impact the mirror performance, are not penalized, mitigating overfitting to strict numerical values.

The weighting factor α is dynamically updated throughout the training, shifting the priority from reflectivity optimization to dispersion correction over time. This enables a staged optimization approach. In the early training phase, lower α values ensure that the model prioritizes reflectivity, whereas in the later training phase, a higher α shifts the focus on fine-tuning the GDD constraints. This dynamic adjustment accelerates convergence, prevents one objective from dominating training, and ensures balanced optimization across reflectivity and dispersion requirements.

3. Results

To validate our AI-driven framework, we first confirm its ability to generate basic optical multi-layer designs. The model successfully produces standard quarter-wave optical thickness (QWOT) stacks, demonstrating its grasp of basic interference principles. Figures 4(a) and (b) displays reflectance (a) and phase (b) of a standard QWOT design (8.9 μ m (total stack thickness)) calculated using the analytical forward model (dashed blue) together with the AI model design (red) (8.5 μ m (total stack thickness)) obtained for a region of high-reflectance broad-bandwidth target (no GDD target considered) taking identical layer materials (tantalum pentoxide ($n \sim 2.08$) and fused silica ($n \sim 1.48$) and number of layers for both designs into account. The optical constants for these materials are based on experimental data obtained from an ion beam sputtering deposition process to ensure a realistic and practical simulation basis which includes material absorption. The AI design displays QWOT-like characteristics reaching a slightly higher maximum reflectance (99.95 %) compared to the QWOT (99.89 %). The slightly improved design found by the AI model indicates that the QWOT is not the optimal design if material absorption is taken into account.

Figures 4(c) and (d) display the reflectance characteristics of two AI-generated designs for other common multi-layer coating challenges. Figure 4(c) illustrates a short pass filter that reflects wavelengths above a selected cut-off wavelength of 600 nm and figure 4(d) illustrates a narrow bandpass filter that selectively transmits a narrow spectral range centered at 720 nm while blocking the surrounding regions. The edge-pass filter reaches > 99.9% reflectivity above 700 nm while effectively blocking wavelengths between 450 and 600 nm, matching the intended spectral characteristics. For all results displayed in figure 4 no expert intervention was necessary and the designs were quickly obtained requiring about a minute of computation time on a consumer-grade GPU (Nvidia 4090 RTX).

Following the performance tests on basic optical coatings, we test the performance of the AI model on a significantly more demanding design. While prior work, such as that by Jiang and Fan [25], has successfully demonstrated the potential of generative models for single-objective problems like antireflection coatings, here we go beyond this by tackling a complex, multi-objective challenge highly relevant to ultrafast laser optics: a broadband, high-reflectivity chirped mirror. The multi-objective target is to achieve high reflectivity (> 99%) over a broad spectral range (940–1120 nm) for p-polarized light at a 5° angle of incidence, while simultaneously ensuring tight GDD control at $-200 \pm 15 \text{ fs}^2$. Our AI model generates a coating design that meets these demanding targets. In figure 5, we show the reflectivity and GDD of this AI-derived layer-stack (solid red lines) and compare our result with state-of-the-art commercially available simulated coatings that target similar performance goals (blue dashed and brown dotted lines). Here, and in the following examples displayed, we use the same material combination: tantalum pentoxide ($n \sim 2.08$) and fused silica ($n \sim 1.48$), considering a wavelength range of 400 nm to 1400 nm.

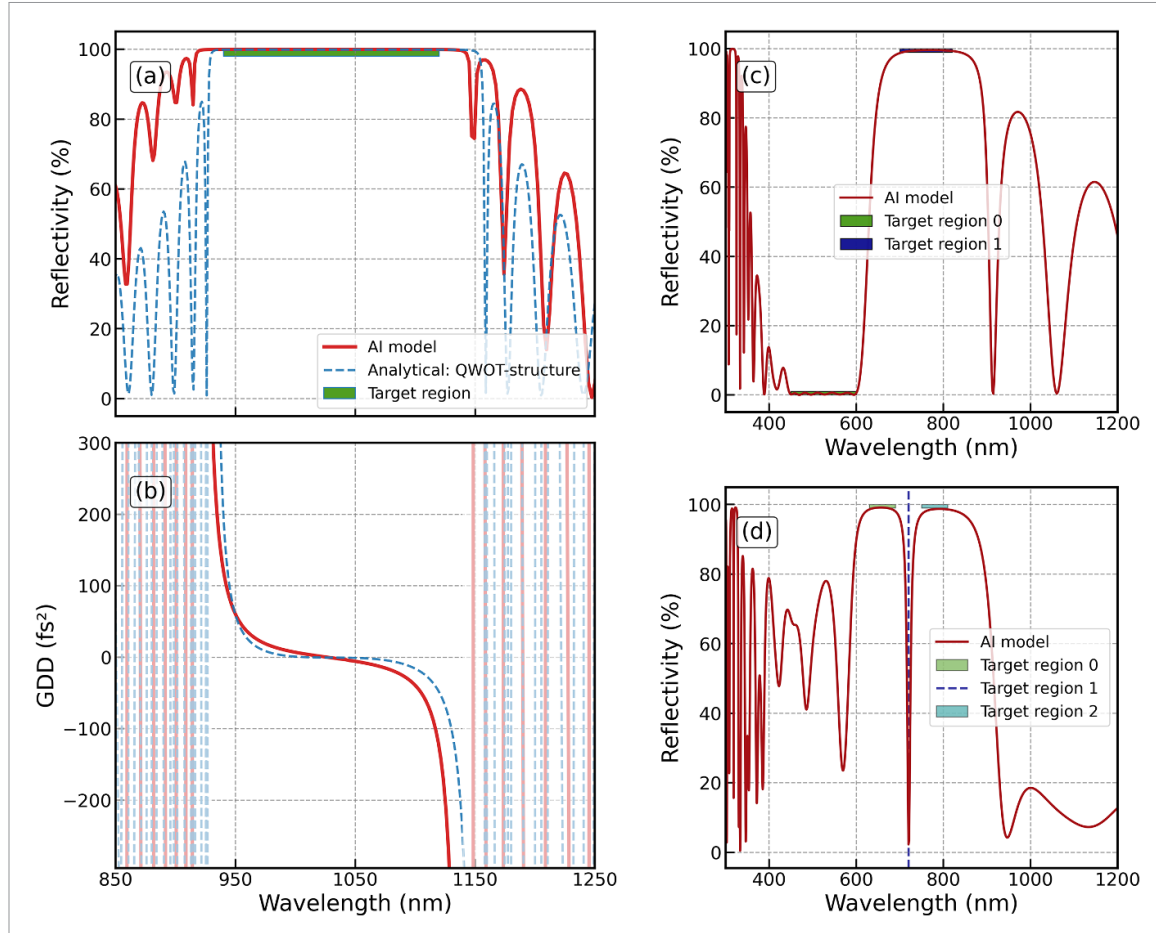


Figure 4. Validation of the AI framework using basic optical coating designs. (a) AI-generated high-reflectance broad-bandwidth mirror and an analytically calculated quarter-wave optical thickness (QWOT) stack (including absorption). (b) Corresponding group delay dispersion (GDD) for the designs displayed in (a). (c) AI-generated edge pass filter, showing a gradual transition from minimum reflectance (passband) to maximum reflectance (stopband). (d) AI-generated narrow bandpass filter featuring high transmission at 720 nm and high reflectance in the surrounding spectral regions.

Our AI-driven model achieves high reflectivity across the target spectral bandwidth while meeting tight GDD demands. However, we notice differences in comparison to the commercial reference designs. As the exact target definition and material properties used for the reference designs are not available, the data presented should not be used to benchmark the performance of the AI model against established coating-design software tools. Instead, the results obtained using the AI model demonstrate the applicability of our framework to demanding coating design problems. In addition, manufacturing tolerances and constraints (e.g. layer deposition errors [32], LIDT [12], etc) have not been explicitly considered in our approach.

In order to provide a more direct comparison and to further evaluate our approach, we used commercial thin-film design software [33]. A comparison between our AI model result and two software derived results is shown in figure 6. Both our AI-generated coating and the commercial software designed coatings are created under identical constraints, i.e. using the same materials (tantalum pentoxide and fused silica) and identical target specifications. Under these conditions, the designs produced by both methods (AI-based and commercial software), compared in figure 6, result in a total physical thickness of approximately 9 μ m each. The resulting layer thickness distribution for our generated design is provided in the supplementary material (figure 7). The same dispersion parameters (refractive index and absorption values) were used in all three cases.

Both reference coatings (dashed blue and dotted brown lines) closely match our AI-generated design in terms of reflectivity and GDD characteristics. These results indicate that our AI-driven approach offers an efficient and automated alternative reaching comparable coating performance characteristics as obtained using state-of-the-art coating design tools.

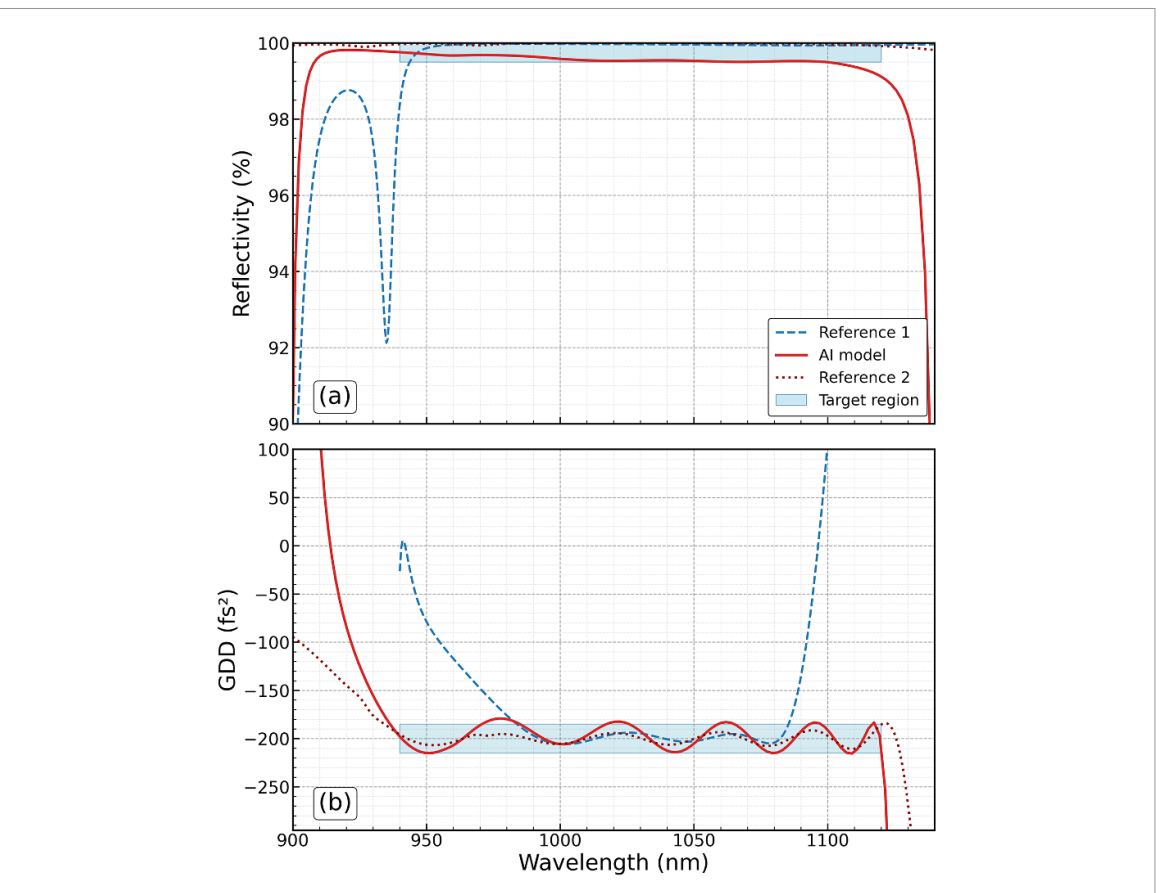


Figure 5. Comparison of AI-designed coating (solid red lines) with state-of-the-art industrial designs (dashed blue and dotted brown lines) for reflectivity (a) and GDD (b). The target reflectivity (>99%) and GDD $(-200 \pm 15 \text{fs}^2)$ used as input for our AI model are indicated by shaded regions.

4. Conclusion and outlook

This study introduces a novel machine-learning-based framework for the design of multilayer optical coatings. By combining an autoencoder-based neural network with a physics-informed loss function, we achieved excellent coating design performance and efficiency. Our AI-driven approach has shown that it can compete with current state-of-the-art optimization techniques. The method does not require expert intervention or adaptation based on physics knowledge of the design process. This opens doors for the automated design of high-performance coatings for ultrafast lasers and other applications. In particular, our approach offers excellent possibilities to enter less explored design parameter spaces and thus offers the potential to find entirely new coating architectures. Although our framework effectively optimizes reflectivity and GDD, future work may incorporate LIDT [12], electric field strength limitations, and manufacturing tolerances [13]. For instance, the LIDT, which is highly dependent on the peak electric field intensity within the multilayer stack, can be integrated as an additional penalty term in our composite loss function. The differentiable physics model can be extended to also calculate this electric field profile, allowing the network to be explicitly penalized for designs that exceed a predefined damage threshold. Future work may also include hybrid approaches that combine our model with data-driven approaches known from classical machine learning that involve training and subsequent inference. This may further enhance the accuracy, speed, and robustness of our design process while offering routes to improved automation and exploitation of unexplored design parameter spaces.

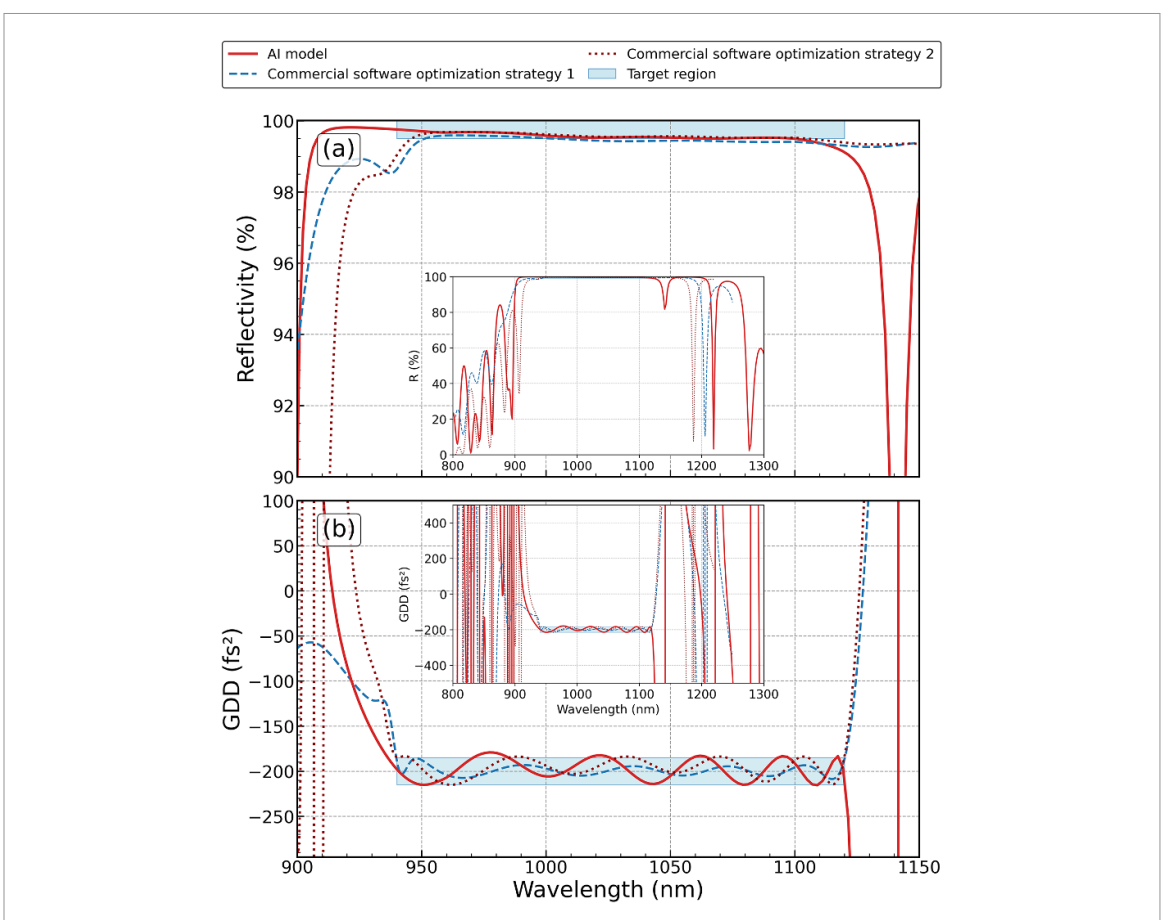


Figure 6. Comparison of the reflectivity (a) and GDD (b) performance of our AI-designed broadband dispersive coating with designs generated using a commercial coating-design software [33]. The inset shows the full spectral performance over a broad wavelength range. Similar target and material properties are considered for all three cases.

Data availability statement

The data cannot be made publicly available upon publication because they contain commercially sensitive information. The data that support the findings of this study are available upon reasonable request from the authors.

Acknowledgments

We acknowledge the support by DASHH (Data Science in Hamburg—Helmholtz Graduate School for the Structure of Matter), as well as DESY (Hamburg, Germany), a member of the Helmholtz Association HGF, for financial support.

Supplementary data

Design details: To provide further details on the coating designs discussed in this work, we present a comparison of the layer thickness distributions for the three different designs discussed in figure 6: (1) the AI-optimized design proposed in this work, (2) Commercial software design 1 and (3) Commercial software design 2. A key difference between the derived designs is visible in the layer stacks, as visualized in figure 7. Although AI-generated designs exhibit a relatively smooth layer distribution, software-optimized designs include more extreme layer thickness variations. The total thicknesses of the designs shown in figure 7 are 10.1 μ m, 9.34 μ m and 8.98 μ m respectively. For all designs, layer 0 is the incident layer, whereas the layer after the last layer is the substrate material.

Hyperparameter Settings: The neural network encoder and the training process utilize the hyperparameters listed in table 1. We determine these values through a combination of common practices in deep learning and empirical tuning for our specific optical design problem.

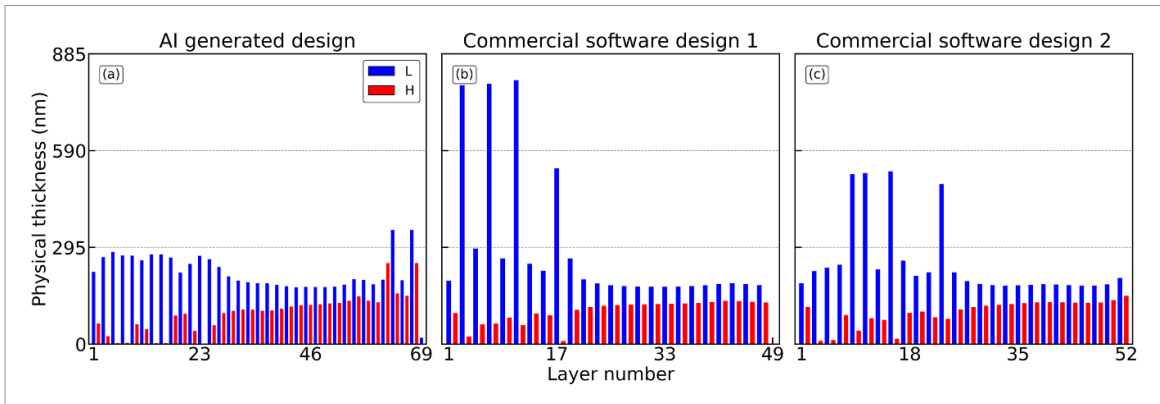


Figure 7. Layer thickness distributions for the coating designs presented in figure 6: (a) AI-optimized design, (b) commercial software design 1, and (c) commercial software design 2. The lower index materials are denoted as L and the higher index material as H.

Table 1. Key hyperparameters for the encoder network and training process.

Hyperparameter	Value
Encoder Architecture	
Hidden layers	3
Neurons per layer	64, 64, 64, [Number of layers in stack]
Activation function	ReLU (hidden), Sigmoid (output)
Output layer scaling	Temperature scaling
Training parameters	
Optimizer	Adam
Learning rate	5×10^{-4}
Batch size	32
Number of epochs	1200

ORCID iDs

Utsa Chattopadhyay © 0009-0006-6570-5820 Florian Carstens © 0000-0002-4841-358X Morten Steinecke © 0000-0002-4124-3039 Tarik Kellermann © 0009-0009-2031-5556 Andreas Wienke © 0000-0002-8927-6534 Ingmar Hartl © 0000-0001-7274-754X Nihat Ay © 0000-0002-8527-2579 Christoph M Heyl © 0000-0003-2133-5224 Henrik Tünnermann © 0000-0002-3850-0356

References

- [1] Ristau D 2005 Optical coatings thin film optical coatings *Encyclopedia of Modern Optics* ed R D Guenther (Elsevier) pp 360–9 (available at: www.sciencedirect.com/science/article/pii/B0123693950008800)
- [2] Zuppella P, Chioetto P, Casini C, Nordera S, Cennamo N, Zeni L and Deppo V D 2021 Optical coatings: applications and metrology Eng. Proc. 11 50
- [3] Kim D et al 2022 Ti/TiO2/SiO2 multilayer thin films with enhanced spectral selectivity for optical narrow bandpass filters Sci. Rep. 12 32
- [4] Ohtera Y, Kurniatan D K and Yamada H 2010 Antireflection coatings for multilayer-type photonic crystals *Opt. Express* 18 12 249–12 261
- [5] Macleod H, Macleod A D M and Macleod J 1969 Thin-Film Optical Filters (CRC Press) (available at: https://api.semanticscholar. org/CorpusID:264236126)
- [6] Tikhonravov A V, Trubetskov M K and DeBell G V 1996 Application of the needle optimization technique to the design of optical coatings *Appl. Opt.* 35 5493–508
- [7] Angelov I V, Pechmann M V, Trubetskov M K, Krausz F and Pervak V 2013 Optical breakdown of multilayer thin-films induced by ultrashort pulses at mhz repetition rates Opt. Express 21 31453–61
- [8] Mackay T and Lakhtakia A 2020 The transfer-matrix method in electromagnetics and optics *Synthesis Lectures on Electromagnetics* 1 pp 1–126
- [9] Knittl Z 1976 Optics of Thin Films: An Optical Multilayer Theory (Wiley)
- [10] Heavens O S 1965 Optical Properties of Thin Films (Dover)

- [11] Dai J, Ji X, Niu X, Jiao H, Cheng X, Wang Z and Zhang J 2025 Efficient multi-objective design method for optical coatings Opt. Lasers Eng. 184 108626
- [12] Papernov S 2014 Laser-Induced Damage in Optical Materials ed D Ristau (CRC Press)
- [13] Apfel J H, Matteucci J S, Newnam B E and Gill D H 1976 Role of Electric Field Strength in Laser Damage of Dielectric Multilayers (Los Alamos National Laboratory (LANL)) p 01 (available at: www.osti.gov/biblio/7343455)
- [14] Tikhonravov A V, Trubetskov M K and DeBell G W 2007 Optical coating design approaches based on the needle optimization technique Appl. Opt. 46 704
- [15] Kaiser N 2008 Old rules useful to the designer of optical coatings https://doi.org/10.1002/vipr.200890042
- [16] Coello C, Coello A, Aguirre A H and Zitzler E 2005 Evolutionary Multi-Criterion Optimization (Springer)
- [17] Guo Y, Yaochu J and Olhofer M 2020 A multiobjective evolutionary algorithm for finding knee regions using two localized dominance relationships IEEE Trans. Evol. Comput. 25 145–58
- [18] Gao W, Wang Y, Liu L and Huang L 2021 A gradient-based search method for multi-objective optimization problems Inf. Sci. 578 129–46
- [19] He C, Zhang Y, Gong D and Ji X 2023 A review of surrogate-assisted evolutionary algorithms for expensive optimization problems Expert Syst. Appl. 217 119495
- [20] Piegari A and Flory F 2018 Optical Thin Films and Coatings: From Materials to Applications (Woodhead Publishing)
- [21] Wang H, Zheng Z, Ji C and Guo L J 2021 Automated multi-layer optical design via deep reinforcement learning Mach. Learn.: Sci. Technol. 2 025013
- [22] Youngjoon H and Nicholls D P 2022 Data-driven design of thin-film optical systems using deep active learning Opt. Express 30 22901–10
- [23] Ma T, Wang H and Guo LJ 2024 Optogpt: a foundation model for inverse design in optical multilayer thin film structures Opto-Electron. Adv. 7 240062–240062
- [24] Yesilyurt O, Peana S, Mkhitaryan V, Pagadala K, Shalaev V M, Kildishev A V and Boltasseva A 2023 Fabrication-conscious neural network based inverse design of single-material variable-index multilayer films Nanophotonics 12 993–1006
- [25] Jiaqi J and Fan J A 2021 Multiobjective and categorical global optimization of photonic structures based on resnet generative neural networks Nanophotonics 10 361–9
- [26] Chuwei W, Li S, He D, and Wang L 2022 Is *l*² physics-informed loss always suitable for training physics-informed neural network? (arXiv:2206.02016)
- [27] Chattopadhyay U, Carstens F, Wienke A, Hartl I, Ay N, Heyl C and Tünnermann H 2024 Neural network method for dielectric optical coating design EPI Web Conf. 307 04057
- [28] Bank D, Koenigstein N and Giryes R 2023 Autoencoders Achine Learning for Data Science Handbook: Data Mining and Knowledge Discovery Handbook (Springer International Publishing) pp 353–74
- [29] Umberto M 2022 An Introduction to Autoencoders (arXiv:2201.03898)
- [30] Alexander L, Mahdavi A, Marquardt F and Wankerl H 2022 Tmm-fast, a transfer matrix computation package for multilayer thinfilm optimization: tutorial *J. Opt. Soc. Am. A* 39 1007–13
- [31] Schmidhuber J 2015 Deep learning in neural networks: an overview Neural Netw. 61 85?117
- [32] Gravalidis C, Gioti M, Laskarakis A and Logothetidis S 2004 Real-time monitoring of silicon oxide deposition processes Surface and Coatings Technology (Proc. Symp. G on Protective Coatings and Thin Films-03, of the E-MRS 2003 Spring Conf.) vol 180-181 pp 655–8 (available at: www.sciencedirect.com/science/article/pii/S0257897203012738)
- [33] Tikhonravov A and Trubetskov M 2022 Optilayer thin film software Version 15.88b (available at: www.optilayer.com)